Biomaterials 35 (2014) 9660–9667

Contents lists available at ScienceDirect

Biomaterials

journal homepage: www.elsevier.com/locate/biomaterials

Bone tissue formation with human mesenchymal stem cells and biphasic calcium phosphate ceramics: The local implication of osteoclasts and macrophages

Anne-Laure Gamblin [a, b], Meadhbh A. Brennan [a, b], Audrey Renaud [a, b], Hideo Yagita [c], Frédéric Lézot [a, b, d], Dominique Heymann [a, b, d, e], Valérie Trichet [a, b, d], Pierre Layrolle [a, b, *]

[a] INSERM, UMR957, Nantes, France
[b] Université de Nantes, Nantes Atlantique Universités, Laboratoire de Physiopathologie de la Résorption Osseuse et Thérapie des Tumeurs Osseuses Primitives, Nantes, France
[c] Department of Immunology, Juntendo University School of Medicine, Tokyo 113-8421, Japan
[d] Equipe LIGUE Nationale Contre le Cancer 2012, Nantes, France
[e] CHU, Hôtel Dieu, Nantes, France

ARTICLE INFO

Article history:
Received 30 June 2014
Accepted 9 August 2014
Available online 29 August 2014

Keywords:
Osteoinduction
Foreign body reaction
Osteoclasts
Macrophages
mAb anti-RANKL

ABSTRACT

Human mesenchymal stem cells (hMSC) have immunomodulative properties and, associated with calcium phosphate (CaP) ceramics, induce bone tissue repair. However, the mechanisms of osteoinduction by hMSC with CaP are not clearly established, in particular the role of osteoclasts and macrophages. Biphasic calcium phosphate (BCP) particles were implanted with or without hMSC in the paratibial muscles of nude mice. hMSC increased osteoblastic gene expression at 1 week, the presence of macrophages at 2 and 4 weeks, osteoclastogenesis at 4 and 8 weeks, and osteogenesis at 4 and 8 weeks. hMSC disappeared from the implantation site after 2 weeks, indicating that hMSC were inducers rather than effectors of bone formation. Induced blockage of osteoclastogenesis by anti-Rankl treatment significantly impaired bone formation, revealing the pivotal role of osteoclasts in bone formation. In summary, hMSC positively influence the body foreign reaction by attracting circulating haematopoietic stem cells and inducing their differentiation into macrophages M1 and osteoclasts, thus favouring bone formation.

1. Introduction

Autologous bone grafts are considered the gold standard in bone regeneration because of their osteogenicity, osteoinductivity, osteoconduction and osteointegration characteristics [1]. However, the bone harvesting procedure requires a second surgical site, at which complications have been reported, and the quantity of bone available for grafting is limited.

Synthetic bone substitutes, particularly calcium phosphate (CaP) ceramics, have been proven safe and biocompatible and are widely used to fill bone defects in clinical indications such as dental, maxillofacial and orthopaedic augmentation [2,3]. Despite having a similar chemical composition to bone mineral [1] and possessing osteoconductive properties, CaP ceramics lack the osteogenicity needed to support bone healing in critical size defects [4] thus limiting their clinical use to small bone defects where osteoconduction is sufficient. The use of bone marrow derived mesenchymal stem cells (MSC) in unison with synthetic biomaterial scaffolds may overcome the challenges of autologous bone grafting for the regeneration of large defects. Human MSC (hMSC) are easily isolated, expanded in culture and have the ability to differentiate into multiple lineages such as osteoblasts, chondrocytes and adipocytes [5]. *In vitro*, hMSC cultured on CaP differentiated into osteoblasts even without osteogenic supplements [6] and *in vivo* bone formation is achieved by the use of MSC with ceramic scaffolds in ectopic sites [7] and critical sized defects [8]. In addition to their regenerative properties, MSC are also known to have unique immunoregulatory properties [8,9]. It has been demonstrated that transplanted hMSC promote wound healing by recruitment of host MSC to the wound site [10] and Song and colleagues elegantly showed the homing of bone marrow MSC to ectopic sites for bone formation by using a sex-mismatched dog model [11].

* Corresponding author. INSERM U957, LPRO, Faculty of Medicine, Nantes, France. Tel.: +33 2 72 64 11 43.
E-mail address: pierre.layrolle@inserm.fr (P. Layrolle).

http://dx.doi.org/10.1016/j.biomaterials.2014.08.018

An inflammatory reaction is expected following implantation of a biomaterial such as CaP due to the host response to a foreign body. During the innate inflammatory reaction, monocytes which circulate in the blood become tissue macrophages [12]. There is evidence that MSC can regulate the macrophage M1/M2 balance to the M2, IL-10 producing anti-inflammatory phenotype [13], by secreting some M2 inducers such as interleukine-4 (IL-4), IL-13 [13], IL-6 [14], and prostaglandin E2 [15]. Bone is essential for a functioning immune system since immune cells originate in the bone marrow; however the significance of immune cells to bone tissue formation is less understood. Nonetheless, disordered bone formation occurs in autoimmune diseases and recently it was shown that ablation of macrophages inhibits intramembranous bone healing [16]. The contribution of macrophages to tissue engineered bone formation is unclear however.

While osteoclast activity is generally associated with bone resorption, it has been demonstrated *in vitro* that osteoclasts secrete mediators which induce the migration and osteogenic differentiation of MSC [17]. In addition, the Wnt/BMP signalling pathway and sphingosine-1-phosphate cytokines, secreted by osteoclasts, seem to be implicated in osteoblast precursor recruitment [18]. Furthermore, osteoclast ablation was found to inhibit ectopic bone formation by β-TCP [19]. However, the influence of transplanted MSC on osteoclast activity during *in vivo* bone formation is unknown.

In this study, the hypothesis that transplanted hMSC, associated with BCP granules, can mobilize circulating monocytes thereby favouring bone formation is tested. Specifically, we investigated the interactions of transplanted hMSC, macrophages and osteoclasts in ectopic ossification in nude mice. To further elucidate the contribution of osteoclasts to bone formation, we used an anti-mouse RANKL antibody depleting osteoclast in mice [20].

2. Materials and methods

2.1. Biomaterials

Micro-porous biphasic calcium phosphate (BCP) granules of 0.5–1 mm in size and composed of HA/β-TCP in a ratio of 20/80 in weight were used as received by the supplier (MBCP+®, Biomatlante, Vigneux de Bretagne, France). Briefly, BCP granules were prepared by mixing calcium deficient apatite with organic pore makers, followed by compaction and sintering at 1050 °C. The overall porosity (% vol) was 75 ± 5%, with a pore size distribution of 70% (0–10 μm), 20% (10–100 μm) and 10% (100–300 μm). Aliquots of 40 mg of BCP granules were prepared in Eppendorf centrifuge tubes sterilized by autoclaving at 121 °C for 20 min.

2.2. hMSC isolation and culture

The human bone marrow mesenchymal stem cells (hMSC) were kindly provided by Prof. Markus Rojewski, Institute for Clinical Transfusion Medicine, Ulm, Germany. After receiving informed consent from adult donors, a bone marrow aspiration was performed under local anaesthesia by haematologists. The cells were seeded at low density on treated culture polystyrene flasks (Corning) and cultured in α-modified Eagle's medium (αMEM, LONZA), supplemented with 10% foetal bovine serum (FBS, Lonza), 100 UI/ml penicillin, 100 μg/ml streptomycin. hMSC were isolated by plastic adherence, amplified in culture until passage 4 in a humidified atmosphere at 37 °C and 5% CO_2. hMSC were characterized by flow cytometry as being positive for CD73, CD90, CD105 and negative for CD45. Multipotency was demonstrated by culturing cells in adipogenic, chondrocytic and osteogenic conditions, as previously described [21]. For the preparation of cell-loaded implants, 1.4×10^6 viable hMSC suspended in 70 μL PBS were added to 40 mg sterile BCP particles. The average time between cell seeding and surgery was approximately 1 h.

2.3. In vivo experimental design

All animal handling and surgical procedures were conducted according to European Community Guidelines (2010/63/EU) for the care and use of laboratory animals. An animal experimentation protocol was prepared, submitted and approved by the local Ethic Committee (CEEA.2012.27).

In order to evaluate the influence of transplanted hMSC on bone formation, *Adult nude NMRI Nu/Nu* female mice (4 weeks old, body weight 20 g) were purchased from a professional stock breeder (Janvier Labs, France). The nude mice were kept in Hepa filtered closets with water and food *ad libitum* and were quarantined for a minimum of 10 days prior to surgery. The mice were randomly and equally divided into 2 groups: BCP particles alone (40 mg) and BCP + hMSC (40 mg and 1.4×10^6 viable cells) that were bilaterally implanted in paratibial muscles. Five mice from each treatment group ($n = 5$) were followed for 1, 2, 4 or 8 weeks after surgery. Animals were placed under general anaesthesia by inhalation of isoflurane (2.5% Flucka, 1 L/min) and an intramuscular injection of the analgesic Buprenorphine (Buprecare 60 μL/kg, Axience) was performed 30 min before surgery. A skin incision of 0.5 cm was made for exposing the muscle, and fibres were taken away to create a pocket where BCP granules were inserted. Skin incisions were closed with sutures (Filapeau 4/0, Peters). The mice were euthanized under general anaesthesia by cervical dislocation.

To determine the impact of osteoclastogenesis on bone formation initiated by hMSC, 8 weeks experiments were reproduced in nude mice which received injections of mAb anti-RANKL. RANKL is a key factor for osteoclast differentiation and activation. Anti-RANKL is known to drastically inhibit the formation of TRAP positive multinucleated cells *in vitro* and *in vivo* [20]. *Adult nude NMRI Nu/Nu* female mice ($n = 4$) were implanted with BCP alone (40 mg on left leg) and BCP + hMSC (40 mg and 1.4×10^6 viable cells, on right leg) and treated with a subcutaneous injection (50 μg dose) of antibody anti-mouse RANKL, kindly provided by Prof. Hideo Yagita, Department of Immunology, Juntendo University School of Medicine, Tokyo, three days before implantation. This same injection regime was repeated twice a week and animals were sacrificed after 8 weeks under general anaesthesia by cervical dislocation. Implants were sectioned after euthanasia to perform histology and RNA extraction.

2.4. Histological analysis

The muscles were excised, fixed in 4% paraformaldehyde, decalcified in a PBS solution with 0.5% paraformaldehyde 4.13% EDTA in a microwave decalcifying automat (KOS Histostation) at 46 °C. Samples were then embedded in paraffin and 3 μm thick sections were cut. Three sections through each implant were attained for histological analysis. The sections were stained with Masson's Trichrome and qualitative/quantitative histological evaluations of soft-tissue in-growth and bone formation were performed. Masson's trichrome technique combines hematoxylin for cell nuclei (blue/black), fuchsine for cytoplasm, muscle and erythrocytes (red) and light green solution for collagen (green). The quantity of new bone was measured in separate sections with the software ImageJ. The bone formation was evaluated according to:

Newly formed bone = (bone surface) * 100/[(total implant surface) − (BCP granules surface)]

Tartrate resistant acide phosphatase (TRAP) is highly expressed by osteoclasts and therefore can be used to stain these cells in histological sections. The sections were stained using a commercial TRAP staining kit (Acid Phosphatase Leukocyte Staining Kit, Sigma) following the manufacturer's instructions. Briefly, the staining solution was prepared with Fast Red TR salt (3.9 mM), naphthol AS-TR phosphate disodium salt (2.3 mM), N–N dimethylformamide (68 μM), and L(+)-tartaric acid (100 mM) all diluted in sodium acetate buffer (0.1 M, pH 5.2). Deparaffinised sections were incubated in the solution for 90 min at 37 °C and then counterstained with Mayer's hematoxylin. TRAP-positive stained cells appeared red. Qualitative/quantitative histological evaluations of osteoclasts were then performed.

2.5. In situ hybridization

In situ hybridization using the human-specific repetitive Alu sequence, which comprises approximately 5% of the total human genome was performed for identification of human cells. Sections were deparaffinized and rehydrated in graded series of ethanol and washed with tris buffered saline (TBS) tween 0.05% pH 7.6 three times for 5 min each under gently agitation. Slides were treated with 3% H_2O_2 for 15 min at room temperature (RT) to block endogenous peroxidase activity, followed by three washes with TBS tween 0.05%. Sections were then treated with 10 μg/mL proteinase K (P2308, Sigma Aldrich, France) for 10 min at 37 °C. After a further three washes for 5 min each in TBS tween 0.05%, sections were treated with 0.25% acetic acid in 0.1 M triethanolamine (TEA) pH 8.0 for 20 min at RT under agitation. Pre-hybridization was performed for 3 h at 56 °C in a hybridization buffer containing 4 × SSC (S6639, Sigma Aldrich France), 50% deionized formamide, 1 × Denhardt's solution, 5% dextran sulphate and 100 μg/mL salmon sperm DNA and molecular grade H_2O. Hybridization buffer was replaced by fresh hybridization buffer containing 70 nM DIG-labeled human locked nucleic acid (LNA) Alu probe 5DigN/5′-TCTCGATCTCCTGACCTCATGA-3′/3DigN (Exiqon, Vedbaek, Denmark) and then target DNA and the probe were denatured for 5 min at 95 °C. Hybridization was carried out for 40 h at 56 °C in a wet chamber. Sections were washed twice in 2 × SSC, then twice in 0.5 × SSC at 56 °C for 10 min each time, followed by three washes in TBS tween 0.05%. Finally, the hybridized probe was detected by immunohistochemistry using biotin-SP-conjugated IgG fraction monoclonal mouse anti-digoxin (Jackson Immunoresearch, Baltimore, USA) diluted 1/200 in PBS for 45 min at 37 °C. After three washes in TBS tween 0.05% at RT, streptaperoxidase was added (1/200 in TBS tween 0.05%) for 45 min at 37 °C before diaminobenzidine (DAB) substrate addition (Dako). Sections were counterstained with Gill-2 hematoxylin (Thermo Shandon Ltd, Runcorn, UK) dehydrated and mounted using Pertex (HistoLab Products AB, Sweden).

2.6. Immunohistochemistry

Immunohistochemistry was performed on deparaffinised and rehydrated sections with specific primary antibodies: CD146 antibody (ab75769, rabbit anti-mouse, 1/200, Abcam), F4/80 antibody (MCA4976, rat anti-mouse, 1/200, Serotec), iNOS antibody (ab15323, rabbit anti-mouse, 1/100, Abcam), CD206 antibody (ab64693, rabbit anti-mouse, 1/1000, Abcam), CD68 (MCA1815T, mouse anti-human, 1/100, Abd Serotex). All sections were counterstained using Gill's hematoxylin and mounted using permanent mounting medium. Tissue staining was viewed using Nanozoomer 2.0 Hamamatsu slide scanner.

The CD146 antibody was used to detect pericytes in the histological sections. CD146, also known as Mel-CAM, MUC18, A32 antigen and S-Endo1, is a membrane glycoprotein observed in pericyte that surround the endothelial layers [22]. The F4/80 antibody was used to detect macrophages M0. The antigen, F4/80, is well expressed in macrophages M0 in most tissues of the developing and adult mouse. The iNOS antibody was utilised in this study for the detection of macrophages M1. Inducible nitric oxide synthase (iNOS) is a enzyme catalysing the production of nitric oxide (NO) from L-arginine [23]. The presence of macrophages M2 was detected by the CD206 antibody. CD206, widely known as the mannose receptor (MR) or more precisely MR C type 1 (MRC1) is a type 1 transmenbrane protein involved in innate immunity [24]. The CD68 antibody was used to detect macrophages M0. CD68 is a member of the lysosome-associated membrane protein (LAMP)-1 family [25]. It is a transmembrane glycoprotein highly expressed by monocytes and tissue macrophages [26].

2.7. Quantitative real-time reverse transcription-polymerase chain reaction (RT-PCR)

Implants were sectioned after euthanasia to perform histology and RNA extraction. Thus, each half of implants were transferred into a 1 mL tube with and vigorously shaken to lyse the cells. Phase separation was performed using chloroform. RNA was recovered from the aqueous phase using isopropanol, and this was followed by alcohol precipitation steps. RNA samples (4 μg) were reverse transcribed with Maxima H Minus First Strand cDNA Synthesis Kit (Thermo Scientific) and random primers in a total volume of 20 μL. Quantitative real-time PCR was performed in the CFX96 (Bio-Rad Laboratories) with SYBR Green detection according the manufacturer's recommendations. PCR amplifications involved 39 cycles of 30 s at 98 °C, 15 s at 95 °C and 30 s at 60 °C. Expression of the target gene was normalized to that of the endogenous control ribosomal protein L19. The $2^{-\Delta Ct}$ (Ct: cycle threshold) method was used to calculate the relative expression levels. Gene name symbols with corresponding full names and the list of corresponding primer sequences are indicated in Table 1. The primer sequence used were specific to mouse genome to only evaluate the host cells behaviour.

Relative gene expression for osteoblastic markers, as alkaline phosphatase (*Alp*), Bone sialo protein (*Bsp*) and osteocalcin (*Oc*), for osteoclastic markers, as acid phosphatase tartrate resistant (*Trap*) have been evaluated.

2.8. Statistics

Statistical comparisons of gene target expression and histomorphometry were performed using Two-way ANOVA and Bonferroni post tests in GraphPad Prism 6.0 software. p values <0.05 were considered statistically significant.

3. Results

3.1. Bone formation is increased by transplanted hMSC

Histological analyses showed bone tissue and bone marrow formation at 4 and 8 weeks in all implants consisting of hMSC and BCP granules (bone incidence 5 out of 5) (Fig. 1A). Conversely, there was no bone tissue at 4 weeks and only small quantities of bone formation without the presence of bone marrow at 8 weeks in the BCP group without cells (Fig. 1A). Quantification by histomorphometry revealed a significant increase in bone formation with BCP plus hMSC at 4 and 8 weeks, compared with BCP alone (5 and 10 fold increase respectively, $p < 0.001$, Fig. 1B). Supporting these findings, there was a significant up-regulation in the expression of mouse bone markers, bone sialo protein and osteocalcin, in BCP plus hMSC at 1 week compared to BCP alone (Fig. 1C). In contrast to histological bone detection that increased between 1 and 8 weeks, the gene expression of these bone markers decreased after 1 week. This apparent discrepancy may be explained by the loss of efficiency in RNA extraction from mineral tissue compared to soft tissue.

3.2. Transplanted hMSC disappear from implanted site

The presence of hMSC in the implants was evaluated by *in situ* hybridization on histological sections and by gene expression of the specific human Alu sequence. As illustrated in Fig. 2A, human cells were detected at 1 and 2 weeks within the BCP plus hMSC implants, while they were not detected at 4 weeks. These results were corroborated by the relative gene expression of Alu sequence (Fig. 2B) which detected human cells within BCP plus hMSC implants at 1 and 2 weeks, but with a large decrease of activity between 1 and 2 weeks (2 fold decrease, $p < 0.001$, Fig. 2B). As expected, no human cell transcription was measured in the control group without human cells. Confirming the *in situ* hybridization results, human cell transcription was not detected within the BCP plus hMSC implants at 4 and 8 weeks.

3.3. Osteoclast activity is enhanced by transplanted hMSC

Distribution of osteoclasts at the implantation site was investigated by the TRAP staining. Representative stained sections showed a large production of this resorbing enzyme around the BCP granules (Fig. 3A). Histomorphometry quantification confirmed that hMSC significantly increased osteoclast activity in the implants (more than a 2 fold increase, $p < 0.001$, Fig. 3B). There was an increase in the relative gene expression of the mouse osteoclast markers *Cathk* and *Trap* at 1 and 2 weeks in both the BCP group and BCP + hMSC group; however there was no difference between the two groups.

3.4. Mobilization of macrophages M0 and M1 to the implant site is enhanced by transplanted hMSC

The distribution of first innate immunological cells, macrophages M0 and M1 within the implants was detected in histological

Table 1
Sequences of primers used for real-time PCR analysis of mouse genes.

	Official Symbol	Official full name; *Alias*	Sense primer antisense primer
Osteogenic markers	*Alpl*	Alkaline phosphatase, liver/bone/kidney; *Alp*	CCGGATCCTGACCAAAAAC GCCTTACCCTCATGATGTCC
	Bglap	Bone gamma-carboxyglutamic acid-containing protein; *Oc*	AGACTCCGGCGCTACCTT CAAGCAGGGTTAAGCTCACA
	Ibsp	Integrin-binding sialo protein; *Bsp*	CGGCGATAGTTCCGAAGAGGA CCCCTCAGAATCTTCATTGTTT
Osteoclaetic markers	*Acp5*	Acid phosphatase 5, tartrate resistant; *Trap*	CGTCTCTGCACAGATTGCAT AAGCGCAAACGGTAGTAAGG
	Ctsk	Cathepsin K; *Cathk*	GGAGGCGGCTATATGACCA GGCGTTATACATACAACTTTCATCC
Reference	*Alu*	Alu sequence	TCTCGATCTCCTGACCTCATGA TCATGAGGTCAGGAGATCGAGA
	Rpl19	Ribosomal protein L19	TCGTTGCCGGAAAAACAC AGGTCACCTTCTCAGGCATC

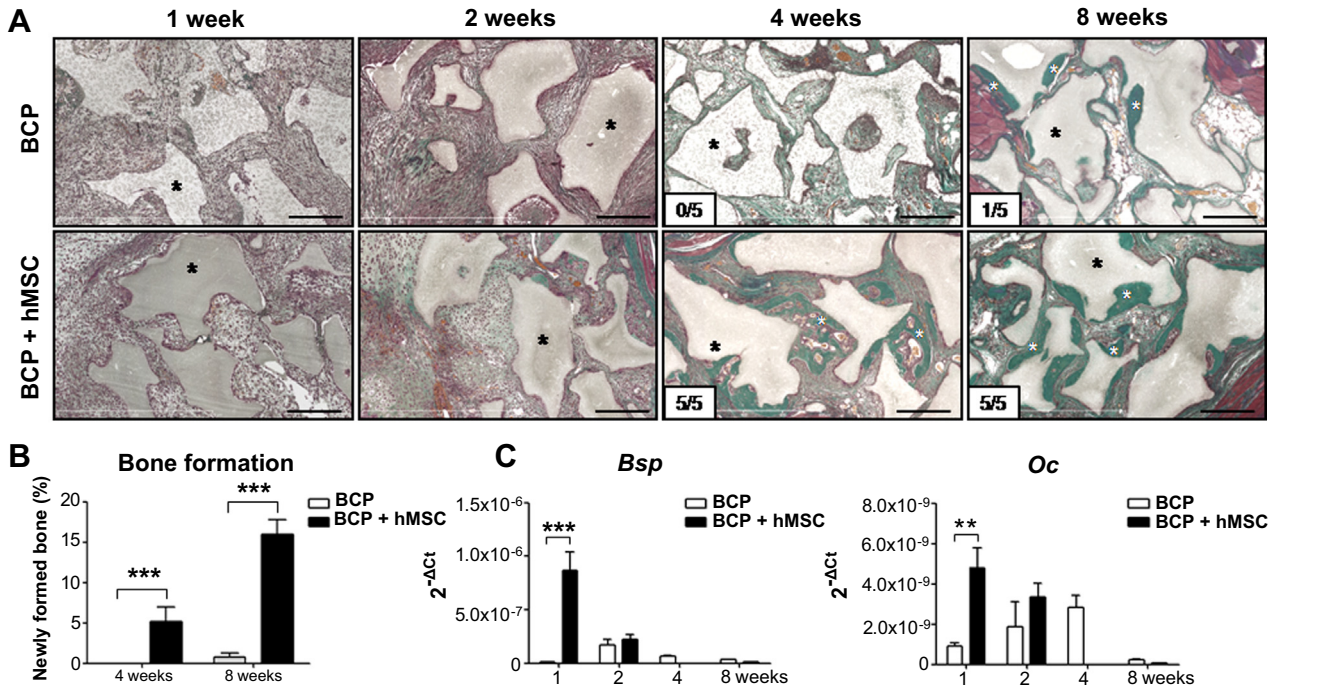

Fig. 1. Ectopic bone formation increased by BCP granules and hMSC. (A) Representative sections stained with Masson's trichrome of BCP granules (black stars) and hMSC implanted in paratibial muscle for 1, 2, 4 and 8 weeks. Ectopic bone formation (white stars) was found in the implants at 4 and 8 weeks. Incidence of bone formation in mice is indicated in white boxes. (B) Percentages of bone formation were evaluated with ImageJ software on the available surface and showed that implantation of human cells increased significantly newly formed bone. ($n = 5$ mice per group, measurement on 3 levels within each total implant, SED, $^{***}p < 0.001$, $^{**}p < 0.01$) (C) Relative gene expression of *Bsp* and *Oc* were evaluated in BCP and BCP + hMSC implants. ($n = 5$ mice per group, SED of triplicate).

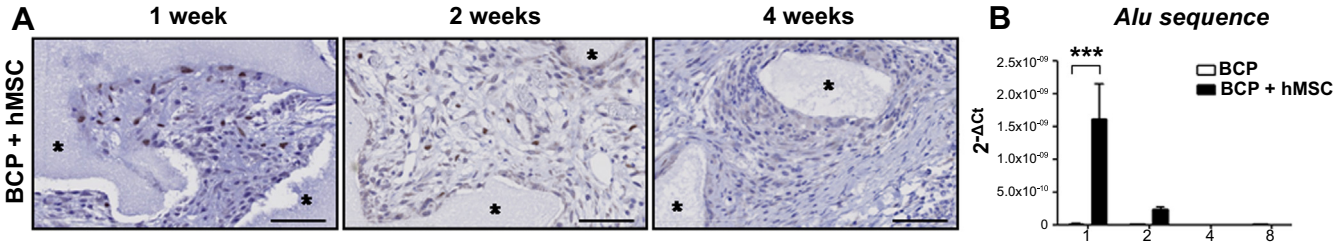

Fig. 2. Disappearence of hMSC after 2 weeks implantation (A) Alu sequence *in situ* hybridization showed human cells were no longer present within the implants at 4 weeks (scale bar = 75 μm). (B) Relative gene expression of Alu sequence decreased over time after implantation. ($n = 5$ mice per group, SED of triplicate $^{***}p < 0.001$).

sections as illustrated in Fig. 4. Macrophages M0, labelled by the antibody anti-F4/80, were distributed in fibrous tissue between the BCP granules, whereas, macrophages M1, labelled by the antibody anti-iNOS, were primarily located surrounding the BCP biomaterial (Fig. 4A). Histomorphological quantification showed an increase in the mobilization of macrophages M0 and M1 to the implant site in the BCP plus hMSC group compared to BCP alone (Fig. 4B). Specifically, macrophages M0 were increased by the presence of hMSC at 2 and 4 weeks and decreased thereafter, while macrophages M1 were significantly higher at 4 weeks as a consequence of hMSC.

Presence of macrophages M2 was investigated by immunohistochemistry directed against CD206 and relative gene expression of CD206, FCGR2, CD163 (data not shown). However, few positive cells were detected and no difference between the BCP alone group and the BCP plus hMSC group was found. The presence of pericytes was also investigated by immunohistochemistry directed against CD146 and relative gene expression of vascular endothelial growth factor and matrix metallopeptidase 2. The implants were highly vascularised but no difference could be quantified between the BCP and BCP + hMSC groups (data not shown). Moreover, CD146 and *in situ* hybridization of Alu sequence were performed on serial sections of each implant demonstrating that human cells did not colocolize in the vessel walls.

3.5. Anti-RANKL treatment induces simultaneous blockage of osteoclastogenesis and reduced bone formation

Fig. 5 depicts 8 week implants in nude mice with or without anti-RANKL treatment which inhibits osteoclastogenesis. Blockage of osteoclast activity was successful with a significant decrease in TRAP staining compared to non-treated controls (Fig. 5A and D). Interestingly, inhibition of osteoclastogenesis with anti-RANKL treatment also resulted in a dramatic reduction in bone formation (from 15% to 5%), as highlighted in Fig. 5B and D. Supporting these results, osteoclastic and osteoblastic gene expression were quantified and showed a considerable decrease with mouse anti-RANKL antibody treatment (Fig. 5E). The distribution of M0 macrophages was studied by immunohistochemistry directed against CD68 (Fig. 5C). The results showed no difference in the presence of macrophages between the untreated and mAb anti-RANKL treated groups.

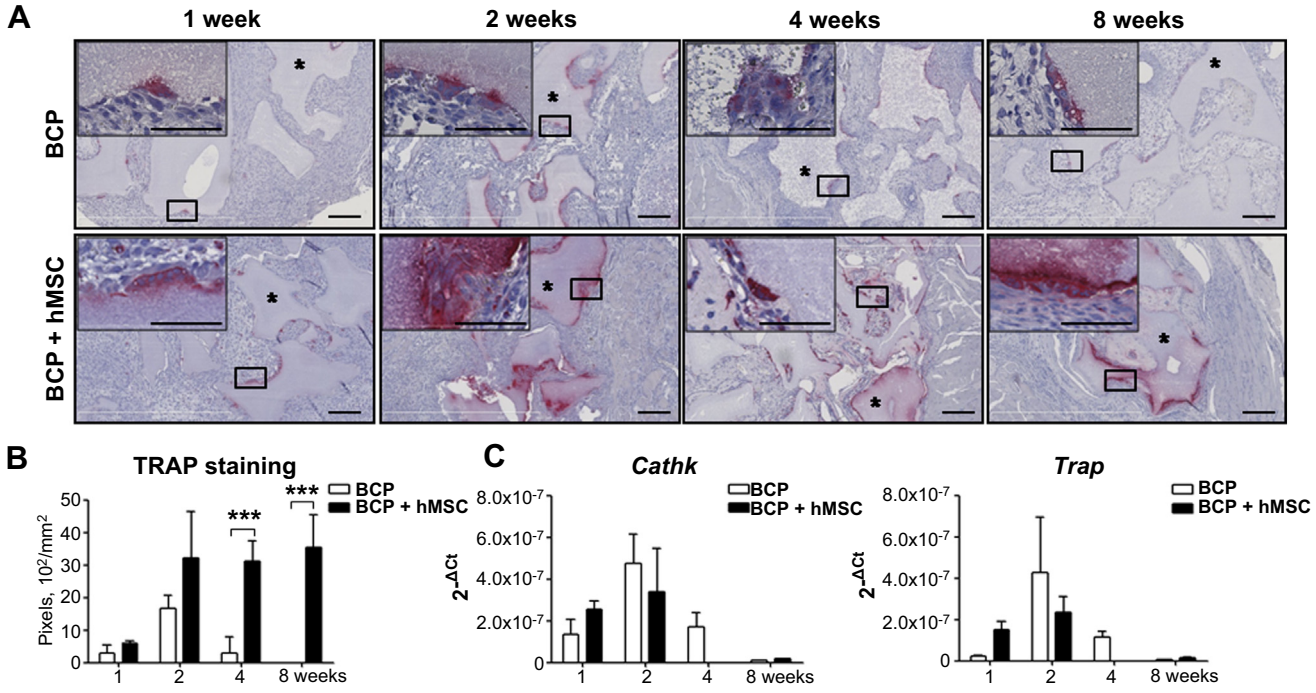

Fig. 3. Osteoclastogenesis increased by BCP granules and hMSC. (A) Representative sections stained for osteoclast marker tartrate resistant acid phosphatase (TRAP, red) showed an increase of multinucleacted TRAP positive cells in BCP plus hMSC implants compared with BCP alone implants. (scale bar = 100 μm) (B) Percentages of TRAP staining were evaluated with ImageJ software on the available surface and showed that implantation of human cells increased significantly the number of osteoclast. ($n = 5$ mice per group, measurement on 3 levels within each total implant, SED, $^{***}p < 0.001$) (C) Relative gene expression of *Cathk* and *Trap* were evaluated in BCP and BCP + hMSC implants. ($n = 5$ mice per group, SED of triplicate). (For interpretation of the references to colour in this figure legend, the reader is referred to the web version of this article.)

4. Discussion

The objective of the present study was to understand the underlying mechanisms of bone formation induced by the grafting of hMSC. To achieve this, micro-porous BCP granules were implanted in the paratibial muscles of nude mice with or without hMSC and the chronological events leading to osteoinduction were identified. Implantation of hMSC considerably enhanced and sped up bone formation. Human cells were not found within the implants at 4 weeks, proving their role as mediators rather than effectors of bone formation. The foreign body reaction was studied revealing that hMSC induced an early mobilization of circulating monocytes to the implantation site as the presence of macrophages and osteoclasts was significantly up-regulated, suggesting their implication in the mechanism of bone formation. To more precisely determine the contribution of osteoclasts to osteogenesis, implantations were repeated in nude mice treated with mAb anti-RANKL to deplete osteoclast formation and activation. Ablation of osteoclastogenesis significantly impaired bone formation, proving the pivotal role of osteoclast-mediated bone formation. The implantation of hMSC with BCP ceramics in this study resulted in a 15 fold increase in bone formation compared to BCP alone. This finding is in agreement with other studies in bone defects [8] and ectopic sites [7] which show the bone-forming benefits of implanted MSC. However, the exact mechanisms by which implanted MSC mediate bone induction is unclear. In the past it was thought that the therapeutic effects of implanted MSC lay in their ability to differentiate into cells of different lineages, into bone-forming osteoblasts in the case of bone tissue engineering. However, in this study the implanted MSC disappeared completely from the implantation site between 2 and 4 weeks and the newly formed bone tissue was exclusively of host origin, suggesting that the implanted MSC facilitate but do not participate directly in the bone formation. Indeed, it has been previously demonstrated that calcium phosphate granules implanted ectopically induced the homing of MSC from the bone marrow to the site of CaP particles implantation to form ectopic bone tissue [11]. Previous studies substantiate the large scale death of implanted MSC [8,27] which is due to ischaemia [25] and lack of glucose [26] in the implant microenvironment. It has recently been shown that the viability of implanted MSC can be maintained in glucose supplemented implants [26]. Nevertheless, the maintained viability of implanted MSC was not necessary to initiate bone formation in this study.

The foreign body reaction against BCP biomaterial and hMSC was investigated in this study and it was found that BCP granules initiated a recruitment of cells of the monocyte/macrophage lineage, which was significantly potentiated by the addition of hMSC. Attraction of macrophages to β-TCP particles was previously demonstrated *in vitro*, whereby macrophages migrated towards the biomaterial by emitting cytoplasmic extensions [28]. Furthermore, interactions of poly morphonuclear neutrophils with hydroxyapatite particles increase levels of pro-inflammatory mediators interleukin-8 (IL-8) and the matrix metallopeptidase 9 [29], a possible mechanism contributing to the mobilization of monocytes and macrophages M1 to BCP. The further significant increase in mobilization of cells of the monocyte lineage by the addition of hMSC in our study, may be explained by the secretion of monocyte chemo-attractant protein-1 by implanted MSC, which was previously described in a model of vascular tissue engineering [30].

It has been previously shown that ablated osteoclastogenesis significantly impaired bone formation by calcium phosphate implantations in ectopic sites [19]. However, the present study is the first to investigate hMSC-mediated osteoclast activity in bone formation. Increased bone formation was found when osteoclast and macrophage M0 and M1 presence was up-regulated at the implantation site by hMSC, and when osteoclastogenesis was abrogated a significant reduction in bone formation was significantly

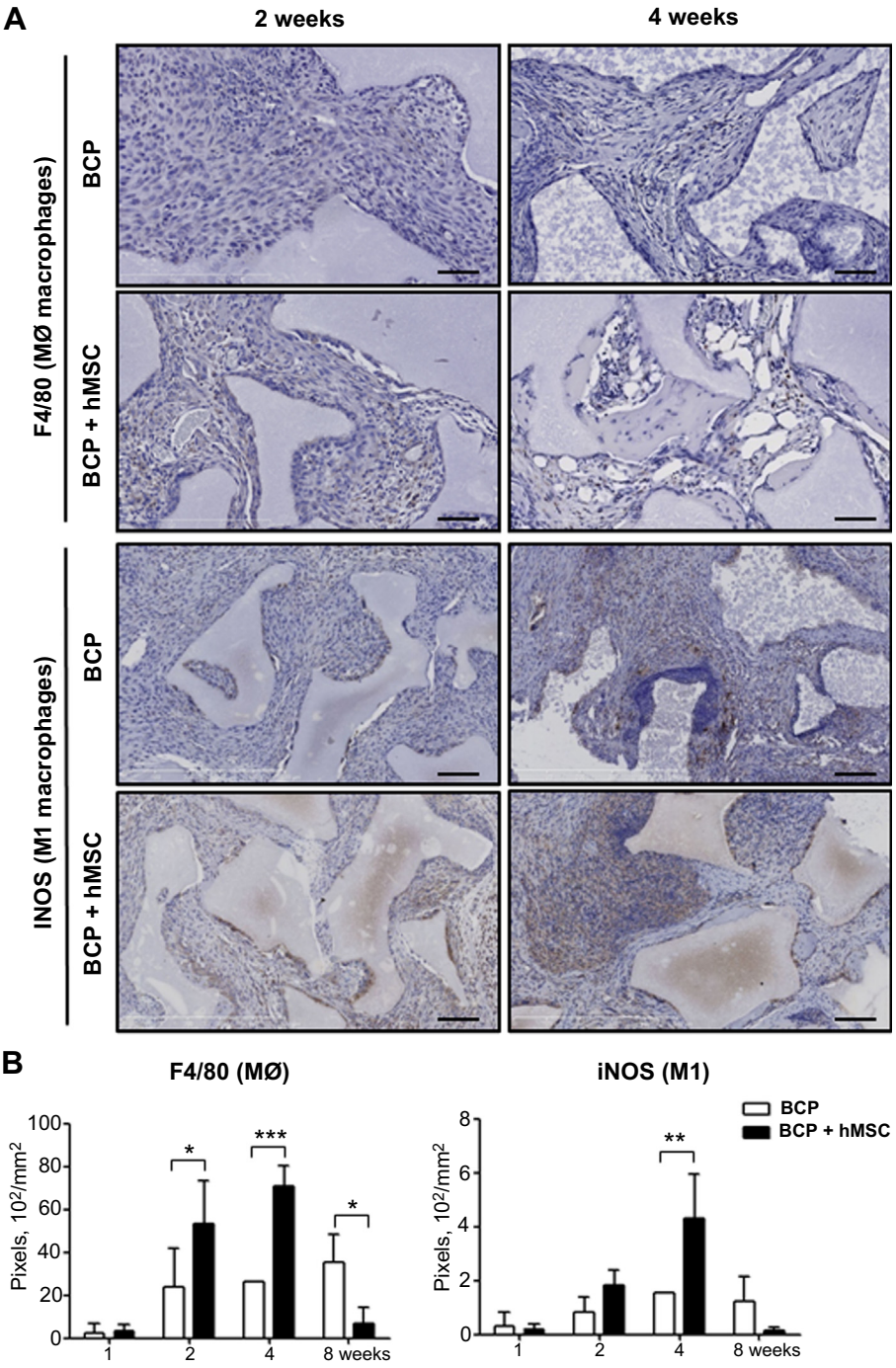

Fig. 4. Mobilization of macrophages M0 and M1 enhanced by transplanted hMSC in nude mice. (A) F4/80 and iNOS immunohistological staining of macrophages showed an increase in mobilization of M0 and M1, respectively, within BCP plus hMSC implants compared to BCP alone (scale bar = 75 μm). (B) Percentages of macrophages M0 and M1 were evaluated with ImageJ software on the available surface. ($n = 5$ mice per group, measurement of 1 mm^2 area on 3 levels within each implant, SED of triplicate, $^{*}p < 0.05$, $^{**}<0.01$, $^{***}<0.001$).

impaired. The precise underlying mechanisms are unclear, however several *in vitro* studies shed light on possible contributing factors such as the secretion of platelet-derived growth factor by osteoclasts which induces the migration of MSC [17] and the production of oncostatin M by monocyte/macrophages and osteoclasts which strongly induces the osteogenic differentiation of MSC *in vitro* [31,32].

In the present study, in response to the implantation of BCP and hMSC, numerous macrophages M0 were observed around the particles and converted into pro-inflammatory M1. Co-implantation with human cells further enhanced this mechanism. Previous studies have shown that MSC can regulate the M1/M2 macrophage balance, favouring a shift towards the M2 anti-inflammatory phenotype [13,15,33]. This move towards the M2 phenotype has been implicated in the resolution of inflammation, tissue repair and remodelling in the heart [34] and kidney [35]. In contrast, the presence of macrophages M2 (study of 3 gene markers by PCR and 1 specific protein by immunohistochemistry), within implants with or without the addition of human cells was not observed in the current study. Therefore, macrophage M2 were shown not to be implicated in MSC mediated

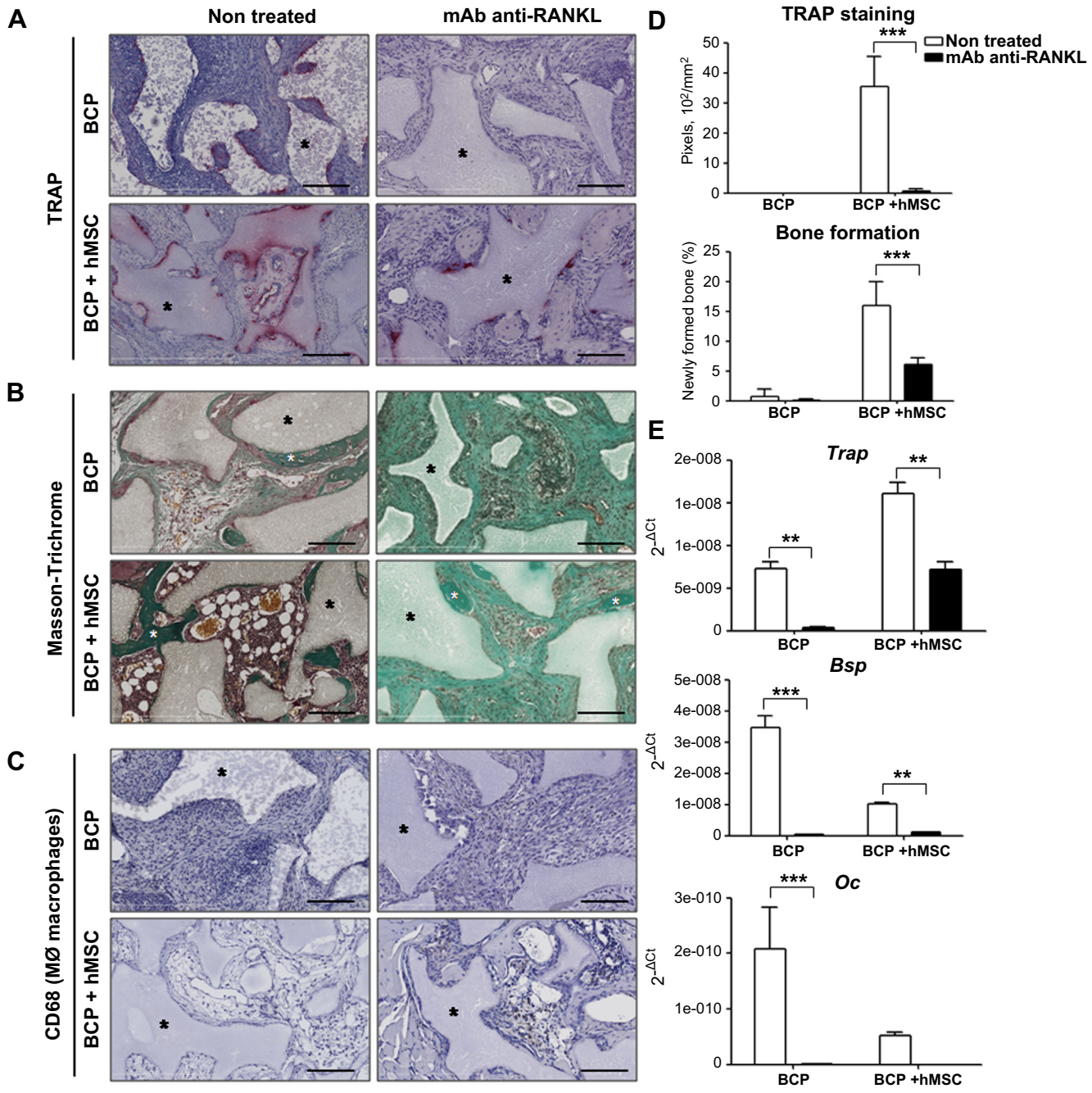

Fig. 5. Ectopic osteoclastogenesis and bone formation were largely decreased with anti-RANKL treatment. (A) Representative sections stained for osteoclast marker TRAP, showed a decrease of multinucleacted TRAP positive cells in anti-RANKL treated mice compared to untreated mice. (B) Representative sections stained with Masson's trichrome of BCP granules (black stars) and BCP + hMSC implanted in paratibial muscle for 8 weeks with or without anti-RANKL treatment. Results showed an important decrease of newly formed bone with mAb treatment (scale bar = 100 μm). (C) Immunohistological staining of CD68 showed no difference in macrophages M0 distribution between control and anti-RANKL groups (scale bar = 100 μm). (D) Percentages of bone formation and osteoclastogenesis were evaluated with ImageJ software on the available surface and showed that treatment decreased significantly newly formed bone and number of osteoclast compared to non-treated group. (E) Relative gene expression of mouse mature bone (*Bsp* and *Oc*) and osteoclast (*Trap*) markers were decreased with anti-RANKL treatment versus control mice with or without human cells ($n = 4$ mice per group, SED of triplicate).

ectopic bone formation, rather macrophages M1 and osteoclasts were the prominent cells implicated in the ectopic osteogenesis mechanism.

It would be interesting to study the macrophage role in bone formation, but independently of the osteoclast one. Alexander et al. have concluded that osteal macrophages promoted bone healing by using clodronate treatment and Macrophage Fas-Induced Apoptosis (MAFIA) transgenic mice model [16]. However, clodronate treatment and conditionally depletion of macrophages in MAFIA alter the osteoclast differentiation as well as the macrophage one. Furthermore, the MAFIA mouse model is in immune-competent mice and the bone formation mechanism should be differently addressed in an immune-deficient model, as suggested by recent study [36].

In this study, the number of vascular cells within the implants was quantified and while the implants were observed to be highly vascularised, no difference between groups was observed. This suggests that there is no direct implication of vascularised tissue in this mechanism of ectopic bone formation induced by BCP granules and hMSC.

5. Conclusion

Human MSC significantly enhanced ectopic bone formation in nude mice. They did not participate directly in osteogenesis, rather they increased the innate immune response and enabled to speed up the mobilization of monocytes to the implantation site where they differentiate into macrophages M1 and osteoclasts. Ablation of osteoclastogenesis by anti-RANKL treatment considerably impaired hMSC-mediated bone formation, highlighting the pivotal role of osteoclasts in the ectopic bone formation. In nude mice models, an up-regulation of osteoclasts and macrophages M1 at the implantation site was correlated with increased bone formation due to hMSC associated to BCP particles.

Acknowledgements

We are very grateful to the members of the European consortium REBORNE in providing the GMP grade cells used to set up the protocols, in particular to Markus Rojewski and Hubert Schrezenmeier from Ulm University. We also thank the company Biomatlante that provided the MBCP+™ granules. This work was supported by the grant (HEALTH-2009-1.4.2-241879) from the 7th Framework Programme of the European Commission REBORNE (Regenerating Bone defects using New biomedical Engineering approaches). ALG is the recipient of a PhD fellowship from the regional council of “Pays de la Loire” (France).

References

[1] Oryan A, Alidadi S, Moshiri A, Maffulli N. Bone regenerative medicine: classic options, novel strategies, and future directions. J Orthop Surg Res 2014;9:18.
[2] Choi H, Park N-J, Jamiyandorj O, Hong M-H, Oh S, Park Y-B, et al. Improvement of osteogenic potential of biphasic calcium phosphate bone substitute coated with synthetic cell binding peptide sequences. J Periodontal Implant Sci 2012;42:166–72.
[3] Nandi SK, Roy S, Mukherjee P, Kundu B, De DK, Basu D. Orthopaedic applications of bone graft & graft substitutes: a review. Indian J Med Res 2010;132:15–30.
[4] Garcia P, Franz D, Raschke M. Bone substitutes - basic principles and clinical applications. Z Orthop Unf 2014;152:152–60.
[5] Fekete N, Rojewski MT, Fürst D, Kreja L, Ignatius A, Dausend J, et al. GMP-compliant isolation and large-scale expansion of bone marrow-derived MSC. PLoS ONE 2012;7:e43255.
[6] Cordonnier T, Langonné A, Corre P, Renaud A, Sensebé L, Rosset P, et al. Osteoblastic differentiation and potent osteogenicity of three-dimensional hBMSC-BCP particle constructs. J Tissue Eng Regen Med 2014;8:364–76.
[7] Veronesi E, Murgia A, Caselli A, Grisendi G, Piccinno MS, Rasini V, et al. Transportation conditions for prompt use of ex vivo expanded and freshly harvested clinical-grade bone marrow mesenchymal stromal/stem cells for bone regeneration. Tissue Eng Part C Methods 2014;20:239–51.
[8] Tour G, Wendel M, Tcacencu I. Bone marrow stromal cells enhance the osteogenic properties of hydroxyapatite scaffolds by modulating the foreign body reaction. J Tissue Eng Regen Med 2012. http://dx.doi.org/10.1002/term.1574.
[9] Le Blanc K, Mougiakakos D. Multipotent mesenchymal stromal cells and the innate immune system. Nat Rev Immunol 2012;12:383–96.
[10] Shin L, Peterson DA. Human mesenchymal stem cell grafts enhance normal and impaired wound healing by recruiting existing endogenous tissue stem/progenitor cells. Stem Cells Transl Med 2013;2:33–42.
[11] Song G, Habibovic P, Bao C, Hu J, van Blitterswijk CA, Yuan H, et al. The homing of bone marrow MSCs to non-osseous sites for ectopic bone formation induced by osteoinductive calcium phosphate. Biomaterials 2013;34:2167–76.
[12] Grage-Griebenow E, Flad HD, Ernst M. Heterogeneity of human peripheral blood monocyte subsets. J Leukoc Biol 2001;69:11–20.
[13] Adutler-Lieber S, Ben-Mordechai T, Naftali-Shani N, Asher E, Loberman D, Raanani E, et al. Human macrophage regulation via interaction with cardiac adipose tissue-derived mesenchymal stromal cells. J Cardiovasc Pharmacol Ther 2013;18:78–86.
[14] Nakajima H, Uchida K, Guerrero AR, Watanabe S, Sugita D, Takeura N, et al. Transplantation of mesenchymal stem cells promotes an alternative pathway of macrophage activation and functional recovery after spinal cord injury. J Neurotrauma 2012;29:1614–25.
[15] Németh K, Leelahavanichkul A, Yuen PST, Mayer B, Parmelee A, Doi K, et al. Bone marrow stromal cells attenuate sepsis via prostaglandin E(2)-dependent reprogramming of host macrophages to increase their interleukin-10 production. Nat Med 2009;15:42–9.
[16] Alexander KA, Chang MK, Maylin ER, Kohler T, Müller R, Wu AC, et al. Osteal macrophages promote in vivo intramembranous bone healing in a mouse tibial injury model. J Bone Min Res 2011;26:1517–32.
[17] Kreja L, Brenner RE, Tautzenberger A, Liedert A, Friemert B, Ehrnthaller C, et al. Non-resorbing osteoclasts induce migration and osteogenic differentiation of mesenchymal stem cells. J Cell Biochem 2010;109:347–55.
[18] Pederson L, Ruan M, Westendorf JJ, Khosla S, Oursler MJ. Regulation of bone formation by osteoclasts involves Wnt/BMP signaling and the chemokine sphingosine-1-phosphate. Proc Natl Acad Sci U S A 2008;105:20764–9.
[19] Davison NL, Gamblin A-L, Layrolle P, Yuan H, de Bruijn JD, Barrère-de Groot F. Liposomal clodronate inhibition of osteoclastogenesis and osteoinduction by submicrostructured beta-tricalcium phosphate. Biomaterials 2014;35:5088–97.
[20] Kamijo S, Nakajima A, Ikeda K, Aoki K, Ohya K, Akiba H, et al. Amelioration of bone loss in collagen-induced arthritis by neutralizing anti-RANKL monoclonal antibody. Biochem Biophys Res Commun 2006;347:124–32.
[21] Redaelli S, Bentivegna A, Foudah D, Miloso M, Redondo J, Riva G, et al. From cytogenomic to epigenomic profiles: monitoring the biologic behavior of in vitro cultured human bone marrow mesenchymal stem cells. Stem Cell Res Ther 2012;3:47.
[22] Li Q, Yu Y, Bischoff J, Mulliken JB, Olsen BR. Differential expression of CD146 in tissues and endothelial cells derived from infantile haemangioma and normal human skin. J Pathol 2003;201:296–302.
[23] Knowles RG, Moncada S. Nitric oxide synthases in mammals. Biochem J 1994;298(Pt 2):249–58.
[24] He L-Z, Crocker A, Lee J, Mendoza-Ramirez J, Wang X-T, Vitale LA, et al. Antigenic targeting of the human mannose receptor induces tumor immunity. J Immunol 2007;178:6259–67.
[25] Becquart P, Cambon-Binder A, Monfoulet L-E, Bourguignon M, Vandamme K, Bensidhoum M, et al. Ischemia is the prime but not the only cause of human multipotent stromal cell death in tissue-engineered constructs in vivo. Tissue Eng Part A 2012;18:2084–94.
[26] Deschepper M, Manassero M, Oudina K, Paquet J, Monfoulet L-E, Bensidhoum M, et al. Proangiogenic and prosurvival functions of glucose in human mesenchymal stem cells upon transplantation. Stem Cells 2013;31:526–35.
[27] Tasso R, Augello A, Boccardo S, Salvi S, Caridà M, Postiglione F, et al. Recruitment of a host's osteoprogenitor cells using exogenous mesenchymal stem cells seeded on porous ceramic. Tissue Eng Part A 2009;15:2203–12.
[28] Beuvelot J, Pascaretti-Grizon F, Filmon R, Moreau M-F, Baslé MF, Chappard D. In vitro assessment of osteoblast and macrophage mobility in presence of β-TCP particles by videomicroscopy. J Biomed Mater Res A 2011;96:108–15.
[29] Velard F, Laurent-Maquin D, Braux J, Guillaume C, Bouthors S, Jallot E, et al. The effect of zinc on hydroxyapatite-mediated activation of human polymorphonuclear neutrophils and bone implant-associated acute inflammation. Biomaterials 2010;31:2001–9.
[30] Roh JD, Sawh-Martinez R, Brennan MP, Jay SM, Devine L, Rao DA, et al. Tissue-engineered vascular grafts transform into mature blood vessels via an inflammation-mediated process of vascular remodeling. Proc Natl Acad Sci U S A 2010;107:4669–74.
[31] Fernandes TJ, Hodge JM, Singh PP, Eeles DG, Collier FM, Holten I, et al. Cord blood-derived macrophage-lineage cells rapidly stimulate osteoblastic maturation in mesenchymal stem cells in a glycoprotein-130 dependent manner. PLoS ONE 2013;8:e73266.
[32] Guihard P, Danger Y, Brounais B, David E, Brion R, Delecrin J, et al. Induction of osteogenesis in mesenchymal stem cells by activated monocytes/macrophages depends on oncostatin M signaling. Stem Cells 2012;30:762–72.
[33] Maggini J, Mirkin G, Bognanni I, Holmberg J, Piazzón IM, Nepomnaschy I, et al. Mouse bone marrow-derived mesenchymal stromal cells turn activated macrophages into a regulatory-like profile. PLoS ONE 2010;5:e9252.
[34] Cho D-I, Kim MR, Jeong H, Jeong HC, Jeong MH, Yoon SH, et al. Mesenchymal stem cells reciprocally regulate the M1/M2 balance in mouse bone marrow-derived macrophages. Exp Mol Med 2014;46:e70.
[35] Eirin A, Zhu X-Y, Li Z, Ebrahimi B, Zhang X, Tang H, et al. Endothelial outgrowth cells shift macrophage phenotype and improve kidney viability in swine renal artery stenosis. Arterioscler Thromb Vasc Biol 2013;33:1006–13.
[36] Bouvet-Gerbettaz S, Boukhechba F, Balaguer T, Schmid-Antomarchi H, Michiels J-F, Scimeca J-C, et al. Adaptive immune response inhibits ectopic mature bone formation induced by BMSCs/BCP/plasma composite in immune-competent mice. Tissue Eng Part A 2014 [in press].